Earth and Planetary Science Letters 454 (2016) 225–236

Contents lists available at ScienceDirect

Earth and Planetary Science Letters

www.elsevier.com/locate/epsl

Interglacial responses of the southern Greenland ice sheet over the last 430,000 years determined using particle-size specific magnetic and isotopic tracers

Robert G. Hatfield[a,*], Alberto V. Reyes[b,c], Joseph S. Stoner[a], Anders E. Carlson[a,c], Brian L. Beard[c], Kelsey Winsor[c,d], Bethany Welke[c]

[a] College of Earth, Ocean, and Atmospheric Science, Oregon State University, Corvallis, OR 97331, USA
[b] Department of Earth and Atmospheric Sciences, University of Alberta, Edmonton, Alberta T6G 2E3, Canada
[c] Department of Geoscience, University of Wisconsin-Madison, 1215 West Dayton Street, Madison, WI 53706, USA
[d] Department of Environmental, Earth & Atmospheric Sciences, University of Massachusetts-Lowell, Lowell, MA 01854, USA

ARTICLE INFO

Article history:
Received 16 May 2016
Received in revised form 2 September 2016
Accepted 6 September 2016
Available online 30 September 2016
Editor: M. Frank

Keywords:
South Greenland ice sheet
sediment tracing
radiogenic isotopes
magnetic properties
quaternary climate change
sea-level rise

ABSTRACT

The past behavior of the Greenland ice sheet can provide important insight into climatic thresholds that may initiate and drive major ice-sheet retreat. Particle-size-specific magnetic and Sr–Nd–Pb isotope records from Eirik Ridge sediments south of Greenland track southern Greenland ice sheet (sGIS) erosional signatures over the past ∼430 ka by discriminating changes in sediment source and transport over the Eirik Ridge. Ground-truthed magnetic and isotopic compositions of subglacial silt from south Greenland's Precambrian bedrock terranes constrain independent magnetic and isotopic estimates of Eirik Ridge silt provenance, which in turn indicate that the southern Greenland ice sheet (sGIS) retreated within its present margin during three of the four previous interglaciations over the past ∼430 ka. Retreat of the sGIS was extensive during the Marine Isotope Stage (MIS) 5e, 9, and 11 interglaciations, continuing unabated despite declining insolation during MIS 5e and 9, with near complete deglaciation in MIS 11. Retreat of the sGIS during MIS 7 was minimal, notwithstanding strong insolation forcing, while Holocene retreat slowed shortly after peak insolation. The reconstruction of sGIS retreat during the last five deglacial and interglacial periods suggests that a threshold for extensive sGIS retreat exists between the insolation and CO_2 states of the Holocene and the MIS 5e and 9 interglaciations, with CO_2 exerting a stronger control on sGIS retreat than insolation. Our results also suggest that the extent and stability of the sGIS in the Holocene is anomalous in the context of late-Quaternary interglaciations.

1. Introduction

Future changes in the volume of Earth's ice sheets will have important environmental, economic, and societal impacts. Past climate conditions, including times both warmer and cooler than present, provide a means of assessing ice-sheet thresholds and responses to changes in Earth's radiative budget (Tzedakis et al., 2009; Carlson and Winsor, 2012; Past Interglacials Working Group of PAGES, 2016). The terrestrial geological record provides the most direct evidence for paleo ice-sheet extent and behavior (e.g. Bennike and Björck, 2002; Carlson and Winsor, 2012; Funder et al., 2011), but such records are limited to the last deglaciation, as earlier evidence was largely erased during glacial advance. Marine sediments, in contrast, can provide well-dated evidence of ice-sheet retreat and advance through glacial–interglacial cycles once sediment source signatures are linked to points of ice-sheet discharge (Carlson et al., 2008; Colville et al., 2011; Reyes et al., 2014; White et al., 2016).

Labrador Sea sediments can provide continuous records of ice-sheet and ocean interactions (e.g., Carlson et al., 2008; Evans et al., 2007; Fagel et al., 2002, 2004; Fagel and Hillaire-Marcel, 2006; Innocent et al., 2000; Hillaire-Marcel et al., 1994; Stanford et al., 2006; Stoner et al., 1995; Winsor et al., 2012). Magnetic, geochemical, and radiogenic-isotope records from Eirik Ridge south of Greenland document changes in the sourcing of sediment from Precambrian Greenland (PG) terranes during glacial terminations and interglaciations that can be used to track ablation of the southern Greenland ice sheet (sGIS) and the magnitude of sGIS retreat (Carlson et al., 2008; Colville et al., 2011; Reyes et al., 2014; Stoner et al., 1995). However, a poor understanding of what drives

* Corresponding author.
E-mail address: rhatfiel@ceoas.oregonstate.edu (R.G. Hatfield).

http://dx.doi.org/10.1016/j.epsl.2016.09.014

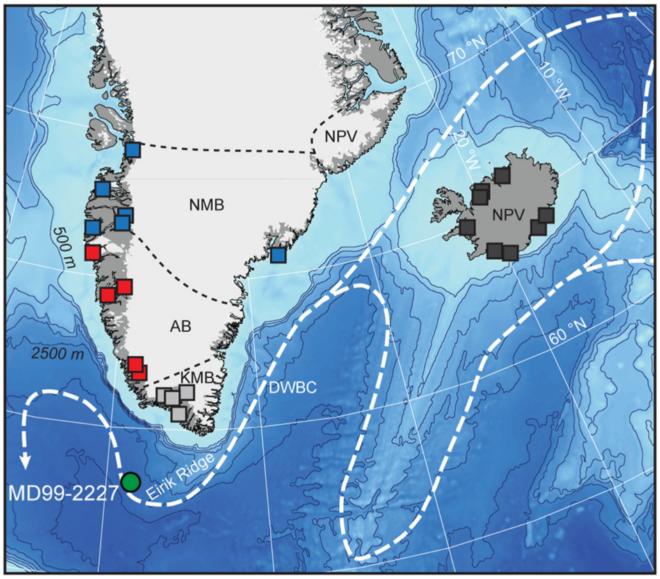

Fig. 1. Location of core MD99-2227 (green circle) and sampling sites of potential terrestrial sediment source terranes (Hatfield et al., 2013; Reyes et al., 2014); KMB, Ketilidian Mobile Belt (grey squares); AB, Archean Block (red squares); NMB, Nagssugtoqidian Mobile Belt (blue squares); NPV, Neogene and Paleogene Volcanics (black squares). Bedrock terrane boundaries are delineated (black dashed lines) and white dashed lines mark the modern-day Deep Western Boundary Current (DWBC) circulation path that is thought to have been active during interglaciations. (For interpretation of the references to color in this figure legend, the reader is referred to the web version of this article.)

bulk magnetic variation over the Eirik Ridge has meant increases in silt proportion and coarsening bulk magnetic grain size in these records have also been interpreted to reflect changes in the transport efficiency of PG and Neogene and Paleogene Volcanic (NPV) sediment from Iceland and East Greenland due to changes in the position and strength of the Deep Western Boundary Current (DWBC) (Evans et al., 2007; Hall et al., 1989; Mazaud et al., 2012; Stanford et al., 2006) (Fig. 1). PG silt sources from the three terranes of southern Greenland, the Ketilidian Mobile Belt (KMB), Archean Block (AB), and Nagssugtoqidian Mobile Belt (NMB), can be discriminated from the NPV (Fig. 1) using silt Sr–Nd–Pb isotope composition, which is controlled by differences in the age and tectonometamorphic history of these terranes (Colville et al., 2011; Reyes et al., 2014). Similarly, the ratio of saturation remanence (Mrs) to saturation magnetization (Ms), as a proxy for ferrimagnetic grain size (Day et al., 1977), has recently shown that PG silt-sized sediments are magnetically coarser (Mrs/Ms range 0.03–0.15) and distinct from the magnetically finer (Mrs/Ms range 0.20–0.32) NPV silts, while their corresponding clay fractions are less easily distinguished (Hatfield et al., 2013).

Because silt-size PG and NPV sediment sources have distinct magnetic (Hatfield et al., 2013) and Sr–Nd–Pb isotopic (Colville et al., 2011; Reyes et al., 2014) signatures, we can isolate the PG signature that can be related to sGIS ablation, sediment export, and retreat, from NPV signatures related to changes to the DWBC (e.g., Fagel et al., 2004; Fagel and Hillaire-Marcel, 2006). We combine new (MIS 10–9 and 8–7) and previously published (MIS 2–1, 6–5e and 12–11; Colville et al., 2011; Reyes et al., 2014) Eirik Ridge silt Sr–Nd–Pb isotope data with new sediment texture data and a new high-resolution magnetic proxy (silt Mrs/Ms) to trace the behavior of the sGIS through the last five glacial terminations and interglaciations. We then compare our independent datasets to changes in radiative forcing since MIS 12 (~430 ka) in order to provide a first record of sGIS response to climate forcing over the last five glacial–interglacial transitions.

2. Materials and methods

2.1. Site setting, age model, and sediment sampling

Our analysis is based on the 43 m sedimentary record from MD99-2227 (58.12°N, 48.22°W, 3460 m water depth) collected during the IMAGES-V Leg II from the Marion Dufresne II. MD99-2227 was cored on the lee side of the southwestern extremity of the Eirik Ridge (Fig. 1) where sediments accumulate rapidly during interglacials in response to a deepening of the DWBC (Hillaire-Marcel et al., 1994; Hunter et al., 2007). Eirik Ridge is a Plio-Pleistocene depositional structure conditioned by sediment redeposition as a result of DWBC flow off south Greenland (Hunter et al., 2007). Subglacial erosion beneath the Greenland, Iceland and Laurentide ice sheets, continental export, and subsequent redistribution by the DWBC delivers abundant terrigenous sediment to Eirik Ridge, with rapidly deposited detrital layers commonly observed during times of ice sheet instability (Hillaire-Marcel et al., 1994; Stoner et al., 1995; Evans et al., 2007; Hunter et al., 2007; Carlson et al., 2008). Lithology reflects these environmental variations and ranges from silty clay with sand and little biogenic material during glacial and deglacial times, to homogeneous nannofossil ooze with silty clay and common bioturbation during interglaciations (Hillaire-Marcel et al., 1994; Fagel and Hillaire-Marcel, 2006; Evans et al., 2007).

Our MD99-2227 age model is based on ^{14}C and δ^{18}O records from planktonic foraminifera and relative (geomagnetic) paleointensity (RPI). We supplement the existing single species (*Neogloboquadrina pachyderma* (sinistral)) MD99-2227 planktonic foraminifera δ^{18}O records (Evans et al., 2007; Reyes et al., 2014; Winsor et al., 2012) for MIS 8–7 and MIS 10–9 with 44 additional analyses of the same single species picked from the 150–250 μm fraction and measured at the Stable Isotope Laboratory at Oregon State University following Winsor et al. (2012). For the glacial–interglaciation intervals MIS 2–1, MIS 6–5, MIS 8–7, and MIS 12–11, we take advantage of published age models. The MIS 2–1 chronology is established using 23 ^{14}C dates for the last ~24 ka (Carlson et al., 2008) while for MIS 6–5, MIS 8–7, and MIS 12–11 it is based on the tandem correlation of RPI (Evans et al., 2007) and the δ^{18}O record of planktic foraminifera (Evans et al., 2007; Reyes et al., 2014; Winsor et al., 2012; this study) to the PISO-1500 RPI and δ^{18}O stacked records (Channell et al., 2009; Reyes et al., 2014). The chronology of PISO-1500 is established by first tuning individual RPI and δ^{18}O records to those of Integrated Ocean Drilling Program (IODP) Site U1308 (Channell et al., 2008, 2009; Hodell et al., 2008). The IODP Site U1308 benthic δ^{18}O record (Hodell et al., 2008) was then tuned to the benthic LR04 δ^{18}O stack (Lisiecki and Raymo, 2005) to generate the PISO-1500 age model (Channell et al., 2009).

Benthic foraminifera are scarce in IODP Site U1308 during the MIS 10–9 interval (Hodell et al., 2008), resulting in chronological uncertainties in the IODP Site U1308 and PISO-1500 age models relative to LR04 during this time interval. Planktic foraminifera are also scarce during Termination 4 (T4) in MD99-2227 (Fig. 2b) making it difficult to establish a chronology through direct tuning of the MD99-2227 δ^{18}O record to LR04 (Fig. 2a). To circumvent this issue, we retune the RPI record of MD99-2227 during MIS 10–9 (Fig. 2d; Evans et al., 2007) to the RPI record of Ocean Drilling Program (ODP) Site 983 (Channell, 1999) on its improved ODP Site 1089 tuned chronology (Stoner et al., 2003) (Fig. 2c). Fifteen tie points were used to generate the MD99-2227 MIS 10–9 age model (Figs. 2c, d). The full, integrated (new and published data), MD99-2227 δ^{18}O record is shown alongside LR04 in Fig. 3.

Using this chronology as a guide, we collected ~3 cm^3 subsamples, typically at 10 cm intervals, between 2400–2990 cm (MIS 8–7) and 3430–3650 cm (MIS 10–9) for magnetic and radiogenic isotope analyses. Sand (>63 μm) was separated by wet sieving;